Smale, S.

Chapter 12

Qualitative dynamics, for cyclists

> **I.1. Introduction to conjugacy problems for diffeomorphisms.** This is a survey article on the area of global analysis defined by differentiable dynamical systems or equivalently the action (differentiable) of a Lie group G on a manifold M. Here Diff(M) is the group of all diffeomorphisms of M and a diffeomorphism is a differentiable map with a differentiable inverse. (...) Our problem is to study the global structure, that is, all of the orbits of M.
>
> Stephen Smale, *Differentiable Dynamical Systems*

In sects. 9.1 and 11.1 we introduced the concept of partitioning the phase space, in any way you please. In chapter 8 we established that stability eigenvalues of periodic orbits are invariants of a given flow. The invariance of stabilities of a periodic orbit is a local property of the flow.

For the Rössler flow of example 3.3, we have learned that the attractor is very thin, but otherwise the return maps that we found were disquieting – figure 3.2 did not appear to be a one-to-one map. This apparent loss of invertibility is an artifact of projection of higher-dimensional return maps onto lower-dimensional subspaces. As the choice of lower-dimensional subspace is arbitrary, the resulting snapshots of return maps look rather arbitrary, too. Other projections might look even less suggestive.

needs expanding!

Such observations beg a question: Does there exist a "natural", intrinsically optimal coordinate system in which we should plot of a return map?

explain return map here

As we shall now argue (see also sect. 17.1), the answer is yes: The intrinsic coordinates are given by the stable/unstable manifolds, and a return map should be plotted as a map from the unstable manifold back onto the immediate neighborhood of the unstable manifold.

In this chapter we show that every equilibrium point and every periodic orbit carries with it stable and unstable manifolds which provide a

stable!manifold
unstable!manifold
manifold!stable
stable!manifold!flow
unstable!manifold, flow
stable!manifold!map
unstable!manifold!map

topologically invariant *global* foliation of the phase space. This qualitative dynamics of stretching and mixing enables us to partition the phase space and assign symbolic dynamics itineraries to trajectories.

Given an itinerary, the topology of stretching and folding fixes the relative spatial ordering of trajectories, and separates the admissible and inadmissible itineraries. The level is distinctly cyclist, in distincition to the pedestrian tempo of the preceeding chapter. Skip this chapter unless you really need to get into nitty-gritty details of symbolic dynamics.

fast track:
chapter 13, p. 213

12.1 Going global: Stable/unstable manifolds

A neighborhood of a trajectory deforms as it is transported by the flow. In the linear approximation, the matrix of variations A describes this shearing of an infinitesimal neighborhood in an infinitesimal time step. The shearing after finite time is described by the Jacobian matrix $\mathbf{J}^t$. Its eigenvalues and eigendirections describe deformation of an initial infinitesimal sphere of neighboring trajectories into an ellipsoid time t later. Nearby trajectories separate exponentially along the unstable directions, approach each other along the stable directions, and maintain their distance along the marginal directions.

The fixed or periodic point x^* stability matrix $\mathbf{J}_p(x^*)$ eigenvectors (8.9) form a rectilinear coordinate frame in which the flow into, out of, or encircling the fixed point is linear in the sense of sect. 4.2. These eigendirections are numerically continued into global curvilinear invariant manifolds as follows.

The global continuations of the local stable, unstable eigendirections are called the *stable*, respectively *unstable manifolds*. They consist of all points which march into the fixed point forward, respectively backward in time

$$\begin{aligned} W^s &= \left\{x \in \mathcal{M} : f^t(x) - x^* \to 0 \text{ as } t \to \infty\right\} \\ W^u &= \left\{x \in \mathcal{M} : f^{-t}(x) - x^* \to 0 \text{ as } t \to \infty\right\} . \end{aligned} \tag{12.1}$$

The stable/unstable manifolds of a flow are rather hard to visualize, so as long as we are not worried about a global property such as the number of times they wind around a periodic trajectory before completing a parcourse, we might just as well look at their Poincaré section return maps. Stable, unstable manifolds for maps are defined by

define y^*; note 2-dimensional only example

$$\begin{aligned} W^s &= \{x \in \mathcal{P} : f^n(x) - x^* \to 0 \text{ as } n \to \infty\} \\ W^u &= \left\{x \in \mathcal{P} : f^{-n}(x) - x^* \to 0 \text{ as } n \to \infty\right\} . \end{aligned} \tag{12.2}$$

For $n \to \infty$ any finite segment of W^s, respectively W^u converges to the linearized map eigenvector $\mathbf{e}^{(e)}$, respectively $\mathbf{e}^{(c)}$. In this sense each eigenvector defines a (curvilinear) axis of the stable, respectively unstable manifold.

Conversely, we can use an arbitrarily small segment of a fixed point eigenvector to construct a finite segment of the associated manifold. Precise construction depends on the type of the eigenvalue(s).

Expanding real and positive eigendirection. Consider ith expanding eigenvalue, eigenvector pair $(\Lambda_i, \mathbf{e}_i)$ computed from $\mathbf{J}$ evaluated at a cycle point,

$$\mathbf{J}(x)\mathbf{e}_i(x) = \Lambda_i \mathbf{e}_i(x)\,, \quad x \in p\,, \quad \Lambda_i > 1\,. \tag{12.3}$$

Take an infinitesimal eigenvector $\epsilon\,\mathbf{e}_i(x)$, $\epsilon \ll 1$, and its image $\mathbf{J}_p(x)\epsilon\,\mathbf{e}_i(x) = \Lambda_i \epsilon\,\mathbf{e}_i(x)$. Sprinkle the interval $|\Lambda_i - 1|\epsilon$ with a large number of points x_m, equidistantly spaced on logarithmic scale $\ln|\Lambda_i - 1| + \ln\epsilon$. The successive images of these points $f(x_j)$, $f^2(x_j)$, $\cdots$, $f^m(x_j)$ trace out the curvilinear unstable manifold in direction $\mathbf{e}_i$. Repeat for $-\epsilon\,\mathbf{e}_i(x)$.

Contractiong real, positive eigendirection. Reverse the action of the map backwards in time. This turns a contracting direction into an expanding one, tracing out the curvilinear stable manifold in continuation of $\epsilon\,\mathbf{e}_j$.

Expanding/contracting real negative eigendirection. As above, but every even iterate $f^2(x_j)$, $f^4(x_j)$, $f^6(x_j)$ continues in the direction $\mathbf{e}_i$, every odd one in the direction $-\mathbf{e}_i$.

Complex eigenvalue pair. Construct an orthonormal pair of eigenvectors spanning the plane $\{\epsilon\,\mathbf{e}_j, \epsilon\,\mathbf{e}_{j+1}\}$. Iteration of the annulus between an infinitesimal circle and its image by $\mathbf{J}$ spans the spiralling/circle unstable manifold of the complex eigenvalue pair $\{\Lambda_i, \Lambda_{i+1} = \Lambda_i^*\}$.

⇓PRELIMINARY

Alternatively, one can write down a parametric equation for the stable (unstable) manifold and generate the manifold by integrating the equation.

explain, draw figure

⇑PRELIMINARY

12.2 Horseshoes

If a flow is locally unstable but globally bounded, any open ball of initial points will be stretched out and then folded back. An example is a 3-dimensional invertible flow sketched in figure 11.7 which returns an area of a Poincaré section of the flow stretched and folded into a "horseshoe", such that the initial area is intersected at most twice(see figure 12.4). Run backwards, the flow generates the backward horseshoe which intersects the forward horseshoe at most 4 times, and so forth. Such flows exist, and

⇓PRIVATE

⇑PRIVATE

motivate 1-d maps with this, replace figure 11.7 by hand-drawn version

Rossler@R"ossler system
horseshoe
map!once-folding
Poincar"e!section
return map
map!return
Henon@H"enon!map
Henon@H"enon!map!fixed points
Henon@H"enon!map!inverse
stable!manifold
unstable!manifold
make example for negative b?

are easily constructed - an example is the Rössler system , discussed in example 3.3.

Now we shall construct an example of a locally unstable but globally bounded mapping which returns an initial area stretched and folded into a "horseshoe", such that the initial area is intersected at most twice. We shall refer to such mappings with at most 2^n transverse self-intersections at the nth iteration as the *once-folding* maps.

12.1 page 209

Add Predrag's pictures

3.4 page 57

As an example is afforded by the 2-dimensional *Hénon map*

$$\begin{aligned} x_{n+1} &= 1 - a x_n^2 + b y_n \\ y_{n+1} &= x_n \,. \end{aligned} \tag{12.4}$$

The Hénon map models qualitatively the Poincaré section return map of figure 11.7. For $b = 0$ the Hénon map reduces to the parabola (11.9), and, as shown in sects. 3.4 and 34.1, for $b \neq 0$ it is kind of a fattened parabola; by construction, it takes a rectangular initial area and returns it bent as a horseshoe.

For definitiveness, fix the parameter values to $a = 6$, $b = 0.9$. The map is quadratic, so it has 2 fixed points $x_0 = f(x_0)$, $x_1 = f(x_1)$ indicated in figure 12.1 (a). For the parameter values at hand, they are both unstable.

add exercise

If you start with a small ball of initial points centered around x_1, and iterate the map, the ball will be stretched and squashed along the line W_1^u.

Similarly, a small ball of initial points centered around the other fixed point x_0 iterated backward in time,

$$\begin{aligned} x_{n-1} &= y_n \\ y_{n-1} &= -\frac{1}{b}(1 - a y_n^2 - x_n) \,, \end{aligned} \tag{12.5}$$

sect?

traces out the line W_0^s. W_0^s is the stable manifold of x_0 fixed point, and W_1^u is the unstable manifold of x_1 fixed point, defined in sect. 12.1. Their intersections enclose the crosshatched region $\mathcal{M}_{\cdot}$. Any point outside W_1^u border of $\mathcal{M}_{\cdot}$ escapes to infinity forward in time, while any point outside W_0^s border escapes to infinity backwards in time. In this way the unstable - stable manifolds define topologically, invariant and optimal $\mathcal{M}_{\cdot}$ initial region; all orbits that stay confined for all times are confined to $\mathcal{M}_{\cdot}$.

Iterated one step forward, the region $\mathcal{M}_{\cdot}$ is stretched and folded into a *smale* horseshoe drawn in figure 12.1 (b). The horseshoe fattened parabolla shape is the consequence og the quadratic form x^2 in (12.4). Parameter a controls the amount of stretching, while the parameter b controls the amount of compression of the folded horseshoe. The case $a = 6$, $b = 0.9$ considered here corresponds to strong stretching and weak compression. Label the two forward intersections $f(\mathcal{M}_{\cdot}) \cap \mathcal{M}_{\cdot}$ by $\mathcal{M}_{s\cdot}$, with $s \in \{0, 1\}$, figure 12.1 (b). The horseshoe consists of the two strips $\mathcal{M}_{0\cdot}, \mathcal{M}_{1\cdot}$, and the bent segment that lies entirely outside the W_1^u line. As all points in this

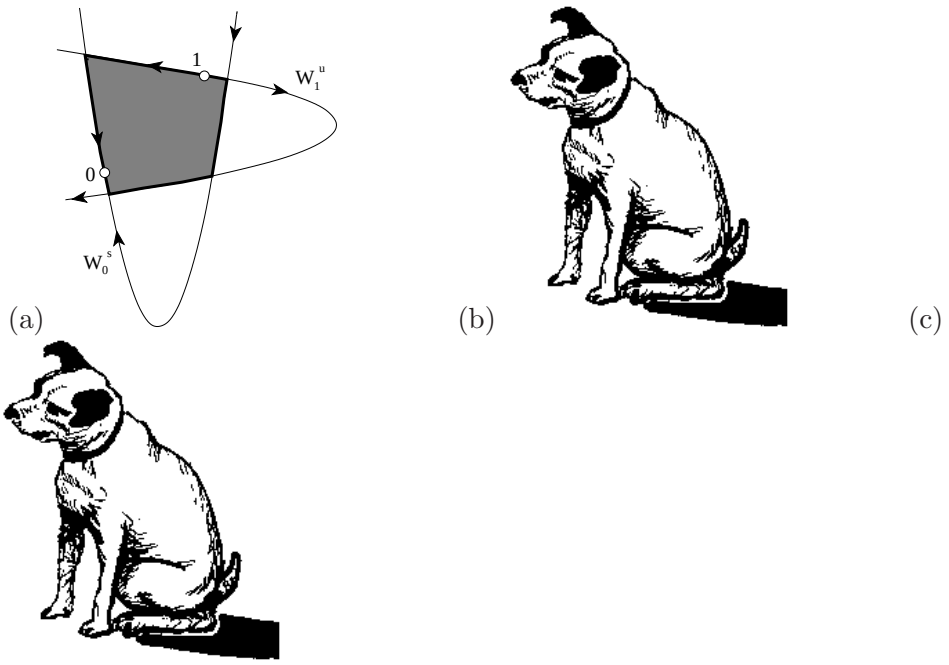

Figure 12.1: The Hénon map for $a = 6$, $b = .9$. (a) The fixed points $\overline{0}$, $\overline{1}$, and the segments of the W_0^s stable manifold, W_1^u unstable manifold that enclose the initial (crosshatched) region $\mathcal{M}_{.}$. (b) The forward horseshoe $f(\mathcal{M}_{.})$. (c) The backward horseshoe $f^{-1}(\mathcal{M}_{.})$. Iteration yields a complete Smale horseshoe, with every forward fold intersecting every backward fold.

segment escape to infinity under forward iteration, this region can safely be cut out and thrown away.

ss forward con-
ion, foliation,
ward ditto

Iterated one step backwards, the region $\mathcal{M}_{.}$ is again stretched and folded into a horseshoe, figure 12.1 (c). As stability and instability are interchanged under time reversal, this horseshoe is transverse to the forward one. Again the points in the horseshoe bend wonder off to infinity as $n \to -\infty$, and we are left with the two (backward) strips $\mathcal{M}_{.0}, \mathcal{M}_{.1}$. Iterating two steps forward we obtain the four strips $\mathcal{M}_{11.}, \mathcal{M}_{01.}, \mathcal{M}_{00.}, \mathcal{M}_{10.}$, and iterating backwards we obtain the four strips $\mathcal{M}_{.00}, \mathcal{M}_{.01}, \mathcal{M}_{.11}, \mathcal{M}_{.10}$ transverse to the forward ones just as for 3-disk pinball game figure 11.3. Iterating three steps forward we get an 8 strips, and so on *ad infinitum*.

What is the significance of the subscript $_{.011}$ which labels the $\mathcal{M}_{.011}$ backward strip? The two strips $\mathcal{M}_{.0}, \mathcal{M}_{.1}$ partition the phase space into two regions labeled by the two-letter alphabet $\mathcal{A} = \{0, 1\}$. $S^+ = .011$ is the *future itinerary* for all $x \in \mathcal{M}_{.011}$. Likewise, for the forward strips all $x \in \mathcal{M}_{s_{-m}\cdots s_{-1}s_0.}$ have the *past itinerary* $S^- = s_{-m}\cdots s_{-1}s_0$. Which partition we use to present pictorially the regions that do not escape in m iterations is a matter of taste, as the backward strips are the preimages of the forward ones

$$\mathcal{M}_{0.} = f(\mathcal{M}_{.0})\,, \qquad \mathcal{M}_{1.} = f(\mathcal{M}_{.1})\,.$$

Ω, the non–wandering set (2.2) of $\mathcal{M}_{.}$, is the union of all points whose

non-wandering set
set!non-wandering
symbolic dynamics!complete
structural stability
stability!structural
horseshoe!complete
structural stability
stability!structural
ordering!spatial

forward and backward trajectories remain trapped for all time. given by the intersections of all images and preimages of $\mathcal{M}$:

$$\Omega = \left\{ x : x \in \lim_{m,n\to\infty} f^m(\mathcal{M}_\cdot) \bigcap f^{-n}(\mathcal{M}_\cdot) \right\} . \tag{12.6}$$

Two important properties of the Smale horseshoe are that it has a *complete binary symbolic dynamics* and that it is *structurally stable*.

For a *complete* Smale horseshoe every forward fold $f^n(\mathcal{M})$ intersects transversally every backward fold $f^{-m}(\mathcal{M})$, so a unique bi-infinite binary sequence can be associated to every element of the non–wandering set. A point $x \in \Omega$ is labeled by the intersection of its past and future itineraries $S(x) = \cdots s_{-2}s_{-1}s_0.s_1s_2\cdots$, where $s_n = s$ if $f^n(x) \in \mathcal{M}_{.s}$, $s \in \{0,1\}$ and $n \in \mathbb{Z}$. For sufficiently separated disks, the 3-disk game of pinball figure 11.3, is another example of a complete Smale horseshoe; in this case the "folding" region of the horseshoe is cut out of the picture by allowing the pinballs that fly between the disks to fall off the table and escape.

The system is said to be *structurally stable* if all intersections of forward and backward iterates of $\mathcal{M}$ remain transverse for sufficiently small perturbations $f \to f + \delta$ of the flow, for example, for slight displacements of the disks, or sufficiently small variations of the Hénon map parameters a, b while structural stability is exceedingly desirable, it is also exceedingly rare. About this, more later.

⇓PRELIMINARY

Inspecting the figure 12.1 (c) we see that the relative ordering of regions with differing finite itineraries is a qualitative, topological property of the flow, so it makes sense to define a simple "canonical" representative partition for the entire class of topologically similar flows.

⇑PRELIMINARY

12.3 Spatial ordering

Consider a system for which you have succeeded in constructing a covering symbolic dynamics, such as a well-separated 3-disk system. Now start moving the disks toward each other. At some critical separation a disk will start blocking families of trajectories traversing the other two disks. The order in which trajectories disappear is determined by their relative ordering in space; the ones closest to the intervening disk will be pruned first. Determining inadmissible itineraries requires that we relate the spatial ordering of trajectories to their time ordered itineraries.

12.9
page 212

So far we have rules that, given a phase space partition, generate a *temporally* ordered itinerary for a given trajectory. Our next task is the reverse: given a set of itineraries, what is the *spatial* ordering of corresponding points along the trajectories? In answering this question we will be aided by Smale's visualization of the relation between the topology of a flow and its symbolic dynamics by means of "horseshoes".

symbol plane@"topp
symbol!square
rectangle
symbol plane@"topp

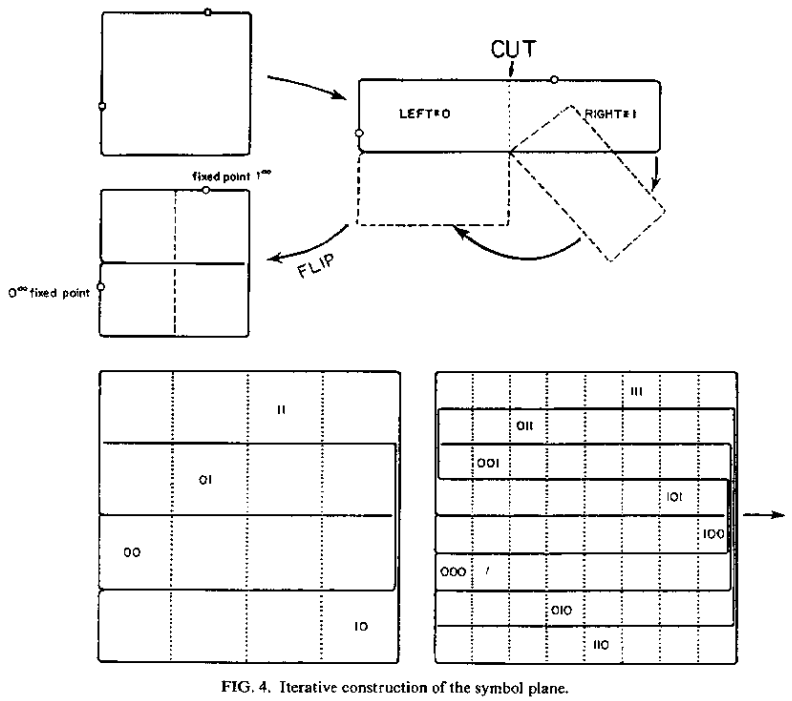

FIG. 4. Iterative construction of the symbol plane.

Figure 12.2: Kneading Danish Pastry: symbol square representation of an orientation reversing once-folding map obtained by fattening the Smale horseshoe intersections of figure 12.1 into a unit square. In the symbol square the dynamics maps rectangles into rectangles by a decimal point shift.

12.3.1 Symbol square

complement figure 12.2 with a figure of rectangles mapping into rectangles

say symbol square is a product of two tent maps

rescan the knife into figure 12.2

For a better visualization of 2-dimensional non–wandering sets, fatten the intersection regions until they completely cover a unit square, as in figure 12.2. We shall refer to such a "map" of the topology of a given "stretch & fold" dynamical system as the *symbol square*. The symbol square is a topologically accurate representation of the non–wandering set and serves as a street map for labeling its pieces. Finite memory of m steps and finite foresight of n steps partitions the symbol square into *rectangles* $[s_{-m+1}\cdots s_0.s_1s_2\cdots s_n]$. In the binary dynamics symbol square the size of such rectangle is $2^{-m}\times 2^{-n}$; it corresponds to a region of the dynamical phase space which contains all points that share common n future and m past symbols. This region maps in a nontrivial way in the phase space, but in the symbol square its dynamics is exceedingly simple; all of its points are mapped by the decimal point shift (11.20)

12.2
page 209

$$\sigma(\cdots s_{-2}s_{-1}s_0.s_1s_2s_3\cdots) = \cdots s_{-2}s_{-1}s_0s_1.s_2s_3\cdots\,, \tag{12.7}$$

For example, the square $[01.01]$ gets mapped into the rectangle $\sigma[01.01] = [010.1]$, see figure 12.4 (b).

⇓PRELIMINARY

As the horseshoe mapping is a simple repetitive operation, we expect a simple relation between the symbolic dynamics labeling of the horseshoe strips, and their relative placement. The symbol square points $\gamma(S^+)$ with

⇑PRELIMINARY
draw a better figure!

12.3
page 209
12.4
page 210

past "topc

future itinerary S^+ are constructed by converting the sequence of s_n's into a binary number by the algorithm (**??**). This follows by inspection from figure 12.2. In order to understand this relation between the topology of horseshoes and their symbolic dynamics, it might be helpful to backtrace to sect. 11.3.2 and work through and understand first the symbolic dynamics of one-dimensional unimodal mappings.

into exercises - orientation preserving case

Under backward iteration the roles of 0 and 1 symbols are interchanged; $\mathcal{M}_0^{-1}$ has the same orientation as $\mathcal{M}$, while $\mathcal{M}_1^{-1}$ has the opposite orientation. We assign to an *orientation preserving* once-folding map the *past topological coordinate* $\delta = \delta(S^-)$ by the algorithm:

12.5 page 210

recheck this

$$
\begin{aligned}
w_{n-1} &= \begin{cases} w_n & \text{if } s_n = 0 \\ 1 - w_n & \text{if } s_n = 1 \end{cases}, \qquad w_0 = s_0 \\
\delta(S^-) &= 0.w_0 w_{-1} w_{-2} \ldots = \sum_{n=1}^{\infty} w_{1-n}/2^n \,. \qquad (12.8)
\end{aligned}
$$

Such formulas are best derived by quiet contemplation of the action of a folding map, in the same way we derived the future topological coordinate (**??**).

The coordinate pair (δ, γ) maps a point (x, y) in the phase space Cantor set of figure 12.1 into a point in the symbol square of figure 12.2, preserving the topological ordering; (δ, γ) serves as a topologically faithful representation of the non–wandering set of any once-folding map, and aids us in partitioning the set and ordering the partitions for any flow of this type.

Include results of refs. [12.65, 12.66]

add chapter on templates, braids?

12.4 Pruning

> The complexity of this figure will be striking, and I shall not even try to draw it.
>
> H. Poincaré, on his discovery of homoclinic tangles, *Les méthodes nouvelles de la méchanique céleste*

In general, not all possible itineraries are realized as physical trajectories. Trying to get from "here" to "there" we might find that a short path is excluded by some obstacle, such as a disk that blocks the path, or a potential ridge. To count correctly, we need to *prune* the inadmissible trajectories, that is, specify the grammar of the admissible itineraries.

While the complete Smale horseshoe dynamics discussed so far is rather straightforward, we had to get through it in order to be able to approach a situation that resembles more the real life: adjust the parameters of a once-folding map so that the intersection of the backward and forward folds is still transverse, but no longer complete, as in figure 13.2 (a). The utility of the symbol square lies in the fact that the surviving, admissible itineraries still maintain the same relative spatial ordering as for the complete case.

replace by the Biham Hénon example

add Henon exercise based on AACI, AACII

pruning!front
subshift!finite type
structural stability
stability!structural
Anosov flows

In the example of figure 13.2 (a) the rectangles [10.1], [11.1] have been pruned, and consequently *any* trajectory containing blocks $b_1 = 101$, $b_2 = 111$ is pruned. We refer to the border of this primary pruned region as the *pruning front*; another example of a pruning front is drawn in figure 13.2 (d). We call it a "front" as it can be visualized as a border between admissible and inadmissible; any trajectory whose periodic point would fall to the right of the front in figure 13.2 is inadmissible, that is, pruned. The pruning front is a complete description of the symbolic dynamics of once-folding maps; we shall discuss this in more depth in sect. 12.5. For now we need this only as a concrete illustration of how pruning rules arise.

⇓PRELIMINARY
⇑PRELIMINARY

In the example at hand there are total of two forbidden blocks 101, 111, so the symbol dynamics is a subshift of finite type (11.24). For now we concentrate on this kind of pruning because it is particularly clean and simple. Unfortunately, for a generic dynamical system a subshift of finite type is the exception rather than the rule. Only some repelling sets (like our game of pinball) and a few purely mathematical constructs (called Anosov flows) are structurally stable - for most systems of interest an infinitesimal perturbation of the flow destroys and/or creates an infinity of trajectories, and specification of the grammar requires determination of pruning blocks of arbitrary length. The repercussions are dramatic and counterintuitive; for example, due to the lack of structural stability the transport coefficients such as the deterministic diffusion constant of sect. 23.2 are emphatically *not* smooth functions of the system parameters. This generic lack of structural stability is what makes nonlinear dynamics so hard; we shall return to the problem of approximating generic infinite Markov partitions in sect. 12.5.

⇓PRELIMINARY
⇑PRELIMINARY

The conceptually simpler finite subshift Smale horseshoes suffice to motivate most of the key concepts that we shall need for time being.

⇓PRELIMINARY

Example 12.1 A Hénon map pruning front:

figure 12.3

$$\det(1-zT) = 1 - t_0 - t_1 - t_{01} + t_0t_1 + t_{01}t_1 + t_0t_{01} - t_{0111} - t_0t_{01}t_1 - t_{00111} + t_0t_{0111} \tag{12.9}$$

$$1/\zeta_{top} = 1 - 2z + 2z^3 - 2z^4$$

Numbers of periodic points (13.25):

$$\begin{aligned}\sum_{n=1} N_n z^n &= \frac{2z - 6z^3 + 8z^4}{1 - 2z + 2z^3 - 2z^4} \\ &= 2z + 4z^2 + 2z^3 + 8z^4 + 12z^5 + 28z^6 + 44z^7 + 80z^8 \\ &\quad +128z^9 + 224z^{10} + 376z^{11} + 656z^{12} + 1120z^{13} + \\ &\quad 1936z^{14} + 3312z^{15} + 5696z^{16} + \ldots \end{aligned} \tag{12.10}$$

⇑PRELIMINARY

subshift!finite type

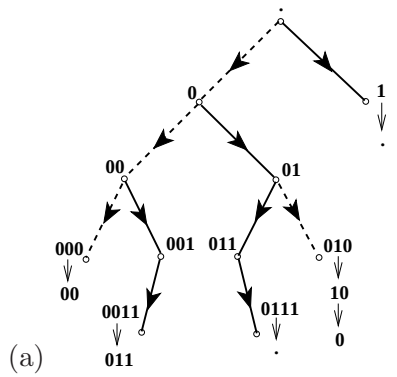

Figure 12.3: Conversion of the pruning front of figure 13.2 (d) into a finite Markov graph. (a) Starting with the start node ".", delineate all pruning blocks on the binary tree. Full line stands for "1" and the dashed line for "0". Label all internal nodes by reading the bits connecting ".", the base of the tree, to the node. The blocks 0010, 0110 are pruned by removing the dashed lines from the 001, 011 nodes. (b) Drop recursively the leading bits in the admissible blocks; if the truncated string corresponds to an internal node in (a), identical trees originate in both, so we connect them. All admissible sequences are generated as walks on this finite Markov graph. (d) Identify all distinct loops and construct the determinant (13.17).

12.4.1 Converting pruning blocks into Markov graphs

The complete binary symbolic dynamics is too simple to be illuminating, so we turn next to the simplest example of pruned symbolic dynamics, the finite subshift obtained by prohibition of repeats of one of the symbols, let us say $_00_$. This situation arises, for example, in studies of the circle maps, where this kind of symbolic dynamics describes "golden mean" rotations (we shall return to this example in chapter 25). Now the admissible itineraries are enumerated by the pruned binary tree of figure 11.13 (a), or the corresponding Markov graph figure 11.13 (b). We recognize this as the Markov graph example of figure 11.14.

13.7 page 235
13.9 page 236

So we can already see the main ingradients of a general algorithm: (1) Markov graph encodes self-similarities of the tree of all itineraries, and (2) if we have a pruning block of length M, we need to descend M levels before we can start identifying the self-similar sub-trees.

Suppose now that, by hook or crook, you have been so lucky fishing for pruning rules that you now know the grammar (11.23) in terms of a finite set of pruning blocks $\mathcal{G} = \{b_1, b_2, \cdots b_k\}$, of lengths $n_{b_m} \leq M$. Our task is to generate all admissible itineraries. What to do?

A Markov graph algorithm.

1. Starting with the root of the tree, delineate all branches that correspond to all pruning blocks; implement the pruning by removing the last node in each pruning block.

2. Label all nodes internal to pruning blocks by the itinerary connecting the root point to the internal node. Why? So far we have pruned

forbidden branches by looking n_b steps into future for all pruning blocks. into future for pruning block $b = [.10010]$. However, the blocks with a right combination of past and future [1.0110], [10.110], [101.10] and [1011.0] are also pruned. In other words, any node whose near past coincides with the begining of a pruning block is potentially dangerous - a branch further down the tree might get pruned.

3. Add to each internal node all remaining branches allowed by the alphabet, and label them. Why? Each one of them is the beginning point of an infinite tree, a tree that should be similar to another one originating closer to the root of the whole tree.

Peles: this one is tricky

4. Pick one of the free external nodes closest to the root of the entire tree, forget the most distant symbol in its past. Does the truncated itinerary correspond to an internal node? If yes, identify the two nodes. If not, forget the next symbol in the past, repeat. If no such truncated past corresponds to any internal node, identify with the root of the tree.

   This is a little bit abstract, so let's say the free external node in question is [1010.]. Three time steps back the past is [010.]. That is not dangerous, as no pruning block in this example starts with 0. Now forget the third step in the past: [10.] is dangerous, as that is the start of the pruning block [10.110]. Hence the free external node [1010.] should be identified with the internal node [10.].

5. Repeat until all free nodes have been tied back into the internal nodes.

6. Clean up: check whether every node can be reached from every other node. Remove the transient nodes, that is, the nodes to which dynamics never returns.

7. The result is a Markov diagram. There is no guarantee that this is the smartest, most compact Markov diagram possible for given pruning (if you have a better algorithm, teach us), but walks around it do generate all admissible itineraries, and nothing else.

Heavy pruning.

describe transients in figure 13.3

We complete this training by examples by implementing the pruning of figure 13.2 (d). The pruning blocks are

$$[100.10], [10.1], [010.01], [011.01], [11.1], [101.10]. \tag{12.11}$$

⇓PRELIMINARY
11.10
page 188
⇑PRELIMINARY

Blocks 01101, 10110 contain the forbidden block 101, so they are redundant as pruning rules. Draw the *pruning tree* as a section of a binary tree with 0 and 1 branches and label each internal node by the sequence of 0's and 1's connecting it to the root of the tree (figure 13.3 (a). These nodes are the potentially dangerous nodes - beginnings of blocks that might end up pruned. Add the side branches to those nodes (figure 13.3 (b). As

transient

we continue down such branches we have to check whether the pruning imposes constraints on the sequences so generated: we do this by knocking off the leading bits and checking whether the shortened strings coincide with any of the internal pruning tree nodes: $00 \to 0$; $110 \to 10$; $011 \to 11$; $0101 \to 101$ (pruned); $1000 \to 00 \to 00 \to 0$; $10011 \to 0011 \to 011 \to 11$; $01000 \to 0$.

As in the previous two examples, the trees originating in identified nodes are identical, so the tree is "self-similar". Now connect the side branches to the corresponding nodes, figure 13.3 (d). Nodes "." and 1 are transient nodes; no sequence returns to them, and as you are interested here only in infinitely recurrent sequences, delete them. The result is the finite Markov graph of figure 13.3 (d); the admissible bi-infinite symbol sequences are generated as all possible walks along this graph.

refer to K.T. Hanson's implementation, Politi?

add Per chapt. 6.1

⇓PRELIMINARY

Include sections of the paper with Kai.

RM: Finite and infinite subshifts. How the above stuff gets complicated. Serious pruning here.

12.5 Pruning dead itineraries

The splitting of cycles into the fundamental cycles and the curvature corrections depends on balancing long cycles t_{ab} against their pseudo-trajectory shadows $t_a t_b$. If the $\overline{ab}$ cycle or either of the shadows $\overline{a}$, $\overline{b}$ do not to exist, such curvature cancellation is unbalanced. In a generic dynamical system not every symbol sequence is realized as a physical trajectory; as one looks further and further, one discovers more and more rules which prohibit families of cycles, with unbalanced curvatures of any length. In the above we have used examples for which all possible orbits can be labeled by all possible binary sequences. In this chapter we discuss the cycle expansions for systems with more complicated symbolic dynamics.

Use 1-d inverse iterates to illustrate that pruning implies existence of complex orbits.

Symbolic dynamics of a generic dynamic system is arbitrarily complex; even for the logistic map the grammar is finite only for special parameter values. Our strategy is akin to bounding a real number by a sequence of rational approximants; we converge toward the non–wandering set under investigation by a sequence of self-similar Cantor sets. A "self-similar" Cantor set (in the sense in which we use the word here) is a Cantor set equipped with a *subshift of finite type* symbol dynamics, that is, the corresponding grammar can be stated as a finite number of pruning rules, each forbidding a finite subsequence $_\epsilon_1\epsilon_2\ldots\epsilon_n_$. Here the notation $_\epsilon_1\epsilon_2\ldots\epsilon_n_$ stands for n consecutive symbols ϵ_1, ϵ_2, ..., ϵ_n, preceeded and followed by arbitrary symbol strings.

The most important lesson of the pruning of the cycle expansions is that prohibition of a finite subsequence unbalances the head of a cycle expansion and increases the number of the fundamental cycles in (18.5). Hence the pruned expansions are expected to start converging only *after* all fundamental cycles have been incorporated - in the last example, the cycles $\overline{1}$, $\overline{10}$, $\overline{10100}$, $\overline{1011100}$. Without cycle expansions, no such crisp and clearcut definition of the fundamental set of scales is available.

A typical Hénon map is not complete. The problem of determining

which symbol sequences are absent, or the problem orbit pruning, viewed in the x-y coordinates, appears formidable. It is equivalent to the problem of determining the location of all homoclinic tangencies, or all turnbacks of the Hénon attractor. They are dense on the attractor, and show no obvious self-similar structure in the x-y plane.

Lozi map!bifurcation
bifurcation!Lozi map

However, in the two dimensional Danish Pastry representation of the attractor, the pruning problem is easily solved; any periodic orbit which contains certain sub-sequence of symbols is forbidden. The forbidden sub-sequences are computed from the map, and are a function of its parameters.

We use the Lozi map to illustrate the orbit pruning problem. The Lozi map has the unstable-pruned orbit structure and non-trivial scaling structure of Hénon type, without the subtleties introduced by the coexistence of stable periodic orbits, or worries about the uniqueness of cycle points corresponding to a given symbol sequence. Furthermore, as the Lozi map is linear, it is computationally fast, and the attractor can be covered by hundreds of thousands of periodic points without straining patience of a desktop workstation.

For the Lozi map (3.14) the stable (unstable) manifolds W^s (W^u) are piecewise linear and easily plotted: figure **??** shows them for parameter values $(a, b) = (1.7, 0.5)$ and $(1.53, 0.5)$. Analysis of the Lozi map is much simpler than that of the Hénon map, as all primary turning points of W^u lie on the line $x = 0$, and the symbol corresponding to a point (x_n, x_{n+1}) is given by the sign of x_{t+1}. An example of a bifurcation of a primary turning point of the Lozi map is sketched in figure **??**.

missing figure **??**

KTH: The three turning points bifurcate together, and a jump of the primary turning point is 0.?

Beyond the orbit pruning and the scaling laws for the allowed unstable orbits, the Hénon attractors also own an infinity of attractive orbits coexisting with the strange attractor. We offer heuristic arguments and solid numerical evidence that the coexistence of attractive orbits does not destroy the strange attractor, which is also in this general case described by the two-dimensional Danish Pastry plot.

12.6 Pruning front

A generic once-folding map does not yield a complete horseshoe; some of the horseshoe pieces might be *pruned*, that is, not realized for particular parameter values of the mapping. In 1 dimension, the criterion for whether a given symbolic sequence is realized by a given unimodal map is easily formulated; any orbit that strays to the right of the value computable from the *kneading sequence* (the orbit of the critical point) is pruned. This is a topological statement, independent of a particular unimodal map. Our objective is to generalize this notion to 2-d once-folding maps.

Our strategy is the following: we first construct a 2-d representation of the covering symbolic dynamics of the map. This is a "road map" in which the various sheets of the stable and unstable manifolds are represented by

straight sections, and the topology is preserved: the nearby periodic points in the symbol square represent nearby periodic points in the phase space. Next we separate the admissible and the forbidden motions by means of a "pruning front", a boundary between the two kinds of orbits.

We make following assumptions:

(i) *The partition conjecture (Grassberger-Kantz) [34.3]:* the non–wandering set of a once-folding map can be described by a subset of a complete Smale horseshoe, partitioned by the set of primary turning points.

(ii) *The pruning-front conjecture (Cvitanović-Gunaratne-Procaccia) [12.21]:* kneading values of the set of all primary turning points separate the admissible from the forbidden orbits, and there are no other pruning rules.

(iii) *Multimodal map approximation [1.3]:* A 2-dimensional once-folding map can be systematically approximated by a sequence of 1-dimensional n-folding maps.

The intuition behind these conjectures is that the folding induced by a single iteration is the primary folding, and all other folds (turnbacks, homoclinic tangencies) are images or preimages of the primary ones. The asymptotic object is a collection of infinitely many 1-d sheets, and the pruning front is the set of the corresponding kneading sequences, one for each 1-d sheet.

Conjectures (i) and (ii) work for all examples that we have studied, and we are not aware of existence of any once-folding maps that contradict them.

Generic symbolic dynamics is not simple - as a matter of fact, already in one dimension its grammar can be arbitrarily complicated. However, the grammar is finite if the critical point is in the basin of attraction of an attractive periodic point; for example, if the critical point is attracted to a stable 3–cycle, the repeller consists of an isolated $\bar{0}$ fixed point and all orbits built from the two letters $\{1, 10\}$, see exercise ?!.

explain golden mean counting for unimodal maps somewhere

The analogous situation can be attained for a 2–dimensional once–folding map if the parameters of the map adjusted so that the intersection of the backward and forward folds is still transverse, but no longer complete, as in figure 13.2 (a). In this particular example the intersections _10.1_, _11.1_ have been lost, and consequently any trajectory containing substrings _101_, _111_ is pruned. We refer to the left border of this primary pruned region as the *pruning front*; an example of a pruning front is drawn in figure 13.2 (d). The pruning front is a 2–dimensional generalization of the 1–dimensional kneading sequence; the location of each vertical step in the pruning front is the kneading sequence of the corresponding primary turnback of the unstable manifolds. When correct, the pruning front conjecture is a complete description of the symbolic dynamics of once-folding maps in the same sense in which the kneading sequence defines the symbolic dynamics of a one–dimensional unimodal map. The intuition behind this conjecture is that the folding induced by a single iteration is the primary folding, and all other folds (turnbacks, homoclinic tangencies) are images or

preimages of the primary ones. The topology puts two obvious constraints on the form of a pruning front:

three-disk@3-disk!pruning front
pruning front!3-disk
Smale, S.
symplectic!transformation
transformation!canonical
transformation!symplectic

1. The pruning front is symmetric across the horizontal 1/2 line.

2. The pruning front is *monotone* across either half of the symbol square.

This is a consequence of the deterministic foliation; inner folds cannot pierce through the outer folds, and therefore have fewer transverse sections than the outer ones.

12.8
page 211

12.7 Hénon map pruning front

Insert table like table 17.2 here for the pruned Hénon map values.

Hénon [3.1] has conjectured that for $(a, b) = (1.4, 0.3)$ the limit cycle of the Hénon map is a *strange attractor*. Its existence has never been proven. While for all practical purposes this is a strange attractor, pruning front techniques that we describe below enable us to find [18.1] stable attractors arbitrarily close by in the parameter space, such as the 13-cycle attractor at $(a, b) = (1.39945219, 0.3)$.

Benedicks and Carleson [12.34] have proven that in the vicinity of $(a, b) = (2, 0)$ strange attractors exist for a Lebesgue measure in the parameter space. PC: recheck the phrasing!

The Danish Pastry transformation, the simplest Baker's transformation appropriate to Hénon type mappings, yields a binary coordinatization of all possible cycle points.

explain Danish Pastry here

The symbolic dynamics of once-folding map is given by the Danish Pastry transformation. This generates both the longitudinal and transverse alternating binary tree. The longitudinal coordinate is given by the head of a symbolic sequence; the transverse coordinate is given by the tail of the symbolic sequence. The dynamics on this space is given by symbol shift permutations; volume preserving, with 2 expansion and 1/2 contraction.

12.8 3-disk pruning front

12.9
page 212
12.10
page 212

Commentary

⇑PRELIMINARY

Remark 12.1 Smale horseshoe. S. Smale understood clearly that the crucial ingredient in the description of a chaotic flow is the topology of its non–wandering set, and he provided us with the simplest visualization of such sets as intersections of Smale horseshoes. In retrospect, much of the material covered here can already be found in Smale's fundamental paper [1.16], but a physicist who has run into a chaotic time series in his laboratory might not know that he is investigating the action (differentiable) of a Lie group G on a manifold M, and that the Lefschetz trace formula is the way to go. If you find yourself mystified by Smale's article abstract about "the action (differentiable) of a Lie group G on a manifold M", quoted on page 191, rereading chapter 9 might help; for example, the Liouville operators form a Lie group (of symplectic, or canonical transformations) acting on the manifold (p, q).

refer also to his biographical notes

kneading!determinant
Markov!partition!infinite

Remark 12.2 Kneading theory. The admissible itineraries are studied in refs. [12.14, 11.8, 11.10, 11.11], as well as many others. We follow here the Milnor-Thurston exposition [12.15]. They study the topological zeta function for piecewise monotone maps of the interval, and show that for the finite subshift case it can be expressed in terms of a finite dimensional *kneading determinant*. As the kneading determinant is essentially the topological zeta function that we introduce in (13.4), we shall not discuss it here. Baladi and Ruelle have reworked this theory in a series of papers [12.17, 12.18, 12.19] and in ref. [12.20] replaced it by a power series manipulation. The kneading theory is covered here in P. Dahlqvist's appendix F.1.

Remark 12.3 Pruning fronts. The notion of a pruning front was introduced in ref. [12.21], and developed by K.T. Hansen for a number of dynamical systems in his Ph.D. thesis [1.3] and a series of papers [12.27]-[12.31]. Detailed studies of pruning fronts are carried out in refs. [12.22, 12.23, 12.52]; ref. [34.5] is the most detailed study carried out so far. The rigorous theory of pruning fronts has been developed by Y. Ishii [12.24, 12.25] for the Lozi map, and A. de Carvalho [12.26] in a very general setting.

Is ref. [34.5] the right one?

refine references, emhasize Carvalho Nonlinearity review

Remark 12.4 The unbearable growth of Markov graphs. A construction of finite Markov partitions is described in refs. [12.56, 12.57], as well as in the innumerably many other references.

If two regions in a Markov partition are not disjoint but share a boundary, the boundary trajectories require special treatment in order to avoid overcounting, see remark F.4 and sect. 22.3.1. If the image of a trial partition region cuts across only a part of another trial region and thus violates the Markov partition condition (11.4), a further refinement of the partition is needed to distinguish distinct trajectories - figure 13.2 is an example of such refinements.

⇓PRELIMINARY
⇑PRELIMINARY
use Mikkelsen termpaper to discuss border points subtleties

The finite Markov graph construction sketched above is not necessarily the minimal one; for example, the Markov graph of figure 13.3 does not generate only the "fundamental" cycles (see chapter 18), but shadowed cycles as well, such as t_{00011} in (13.17). For methods of reduction to a minimal graph, consult refs. [11.5, 12.51, 12.53]. Furthermore, when one implements the time reversed dynamics by the same algorithm, one usually gets a graph of very different topology even though both graphs generate the same admissible sequences, and have the same determinant. The algorithm described here makes some sense for 1-d dynamics, but is unnatural for 2-d maps whose dynamics it treats as one-dimensional. In practice, generic pruning grows longer and longer, and more plentiful pruning rules. For generic flows the refinements might never stop, and almost always we might have to deal with infinite Markov partitions, such as those that will be discussed in sect. 13.6. Not only do the Markov graphs get more and more unwieldy, they have the unpleasant property that every time we add a new rule, the graph has to be constructed from scratch, and it might look very different form the previous one, even though it leads to a minute modification of the topological entropy. The most determined effort to construct such graphs may be the one of ref. [12.22]. Still, this seems to be the best technology available, unless the reader alerts us to something superior.

Résumé

Given a partition $\mathcal{A}$ of the phase space $\mathcal{M}$, a dynamical system $(\mathcal{M}, f)$ induces topological dynamics (Σ, σ) on the space Σ of all admissible bi–infinite itineraries. The itinerary describes the time evolution of an orbit, while (for 2-d hyperbolic maps) the symbol square describes the spatial ordering of points along the orbit. The rule that everything to one side of the pruning front is forbidden might (in hindsight) seem obvious, but if you have ever tried to work out symbolic dynamics of some "generic" dynamical system, you should be struck by its simplicity: instead of pruning a Cantor set embedded within some larger Cantor set, the pruning front cleanly cuts out a *compact* region in the symbol square and that is all - there are no additional pruning rules.

The symbol square is a useful tool in transforming topological pruning into pruning rules for inadmissible sequences; those are implemented by constructing transition matrices and/or Markov graphs. These matrices are the simplest examples of evolution operators prerequisite to developing a theory of averaging over chaotic flows.

Importance of symbolic dynamics is often grossly unappreciated; as we shall see in chapters 16 and 18, coupled with uniform hyperbolicity, the existence of a finite grammar is the crucial prerequisite for construction of zeta functions with nice analyticity properties.

extract parts of refsKnead.tex

References

remember to put improvements back to refs.all

[12.1] E. Hopf, *Ergodentheorie* (Chelsea Publ. Co., New York 1948).

[12.2] E. Hopf, *Abzweigung einer periodischen Lösung*, Beriech. Sächs. Acad. Wiss. Leipzig, Math. Phys. Kl. **94**, 19 (1942), 15-25.

[12.3] T. Bedford, M.S. Keane and C. Series, eds., *Ergodic Theory, Symbolic Dynamics and Hyperbolic Spaces* (Oxford University Press, Oxford, 1991).

[12.4] M.S. Keane, *Ergodic theory and subshifts of finite type*, in ref. [12.3].

[12.5] B. Kitchens, "Symbolic dynamics, group automorphisms and Markov partition", in *Real and Complex Dynamical Systems*, B. Branner and P. Hjorth, ed. (Kluwer, Dordrecht, 1995).

[12.6] R. Bowen, *Markov partitions for Axiom A diffeomorphisms"*, *Amer. J. Math.* **92**, 725 (1970).

[12.7] D. Ruelle, *Transactions of the A.M.S.* **185**, 237 (197?). what year?

[12.8] R. Bowen, *Periodic orbits for hyperbolic flows*, Amer. J. Math. **94**, 1-30 (1972).

[12.9] R. Bowen, *Symbolic dynamics for hyperbolic flows*, Amer. J. Math. **95**, 429-460 (1973).

[12.10] R. Bowen and O.E. Lanford *Math. ??* **??**,

[12.11] R. Bowen and O.E. Lanford, *"Zeta functions of restrictions"*, pp. 43-49 in *Proceeding of the Global Analysis*, (A.M.S., Providence 1968).

[12.12] V.M. Alekseev and M.V. Jakobson, *Symbolic dynamics and hyperbolic dynamical systems*, Physics Reports, **75**, 287, (1981).

[12.13] A. Manning, "Axiom A diffeomorphisms have rational zeta function", *Bull. London Math. Soc.***3**, 215 (1971).

[12.14] A.N. Sarkovskii, "Coexistence of cycles of a continuous map of a line into itself", *Ukrainian Math. J.* **16**, 61 (1964).

[12.15] J. Milnor and W. Thurston, *"On iterated maps of the interval"*, in A. Dold and B. Eckmann, eds., *Dynamical Systems, Proceedings, U. of Maryland 1986-87, Lec. Notes in Math.* **1342,** 465 (Springer, Berlin 1988).

[12.16] W. Thurston, *"On the geometry and dynamics of diffeomorphisms of surfaces"*, *Bull. Amer. Math. Soc.* **19**, 417 (1988).

[12.17] V. Baladi and D. Ruelle, *"An extension of the theorem of Milnor and Thurston on the zeta functions of interval maps"*, *Ergodic Theory Dynamical Systems* **14**, 621 (1994).

[12.18] V. Baladi, *"Infinite kneading matrices and weighted zeta functions of interval maps"*, *J. Functional Analysis* **128**, 226 (1995).

[12.19] D. Ruelle, *"Sharp determinants for smooth interval maps"*, in F. Ledrappier, J. Lewowicz, and S. Newhouse, eds., *Proceedings of Montevideo Conference 1995* (Addison-Wesley, Harlow 1996).

[12.20] V. Baladi and D. Ruelle, *"Sharp determinants"*, *Invent. Math.* **123**, 553 (1996).

[12.21] P. Cvitanović, G.H. Gunaratne and I. Procaccia, *Phys. Rev.* **A 38**, 1503 (1988).

[12.22] G. D'Alessandro, P. Grassberger, S. Isola and A. Politi, "On the topology of the Hénon Map", *J. Phys.* **A 23**, 5285 (1990).

[12.23] G. D'Alessandro, S. Isola and A. Politi, "Geometric properties of the pruning front", *Prog. Theor. Phys.* **86**, 1149 (1991).

[12.24] Y. Ishii, "Towards the kneading theory for Lozi attractors. I. Critical sets and pruning fronts", Kyoto Univ. Math. Dept. preprint (Feb. 1994).

[12.25] Y. Ishii, "Towards a kneading theory for Lozi mappings. II. A solution of the pruning front conjecture and the first tangency problem", *Nonlinearity* **10**, 731 (1997).

[12.26] A. de Carvalho, Ph.D. thesis, CUNY New York 1995; "Pruning fronts and the formation of horseshoes", preprint (1997).

[12.27] K.T. Hansen, *CHAOS* **2**, 71 (1992).

UPDATE! [12.28] K.T. Hansen, *Nonlinearity* **5**

UPDATE! [12.29] K.T. Hansen, *Nonlinearity* **5**

[12.30] K.T. Hansen, *Symbolic dynamics III, The stadium billiard*, to be submitted
UPDATE! to *Nonlinearity*

[12.31] K.T. Hansen, *Symbolic dynamics IV; a unique partition of maps of Hénon type*, in preparation.

[12.32] Fa-Geng Xie and Bai-Lin Hao, "Counting the number of periods in one-dimensional maps with multiple critical points", *Physica A* **202**, 237 (1994).

[12.33] M. Benedicks and L. Carleson, *Ann. of Math.*, **122**, 1 (1985).

[12.34] M. Benedicks and L. Carleson, *IXth Int. Congr. on Mathematical Physics*, B. Simon *et al.*, eds., p.489, (Adam Hilger, Bristol, 1989).

[12.35] M. Benedicks and L. Carleson, *Ann. of Math.* **133**, 73 (1991).

[12.36] G. D'Alessandro and A. Politi, "Hierarchical approach to complexity ...", *Phys. Rev. Lett.* **64**, 1609 (1990).

[12.37] F. Christiansen and A. Politi, "A generating partition for the standard map", *Phys. Rev. E.* **51**, 3811 (1995); `chao-dyn/9411005`

[12.38] F. Christiansen and A. Politi, "Symbolic encoding in symplectic maps", *Nonlinearity* **9**, 1623 (1996).

[12.39] F. Christiansen and A. Politi, "Guidelines for the construction of a generating partition in the standard map", *Physica D* **109**, 32 (1997).

[12.40] T. Hall, "Fat one-dimensional representatives of pseudo-Anosov isotopy classes with minimal periodic orbit structure", *Nonlinearity* **7**, 367 (1994).

[12.41] P. Cvitanović and K.T. Hansen, "Symbolic dynamics of the wedge billiard", Niels Bohr Inst. preprint (Nov. 1992)

[12.42] P. Cvitanović and K.T. Hansen, "Bifurcation structures in maps of Hénon type", *Nonlinearity* **11**, 1233 (1998).

[12.43] R.W. Easton, "Trellises formed by stable and unstable manifolds in plane", *Trans. Am. Math. Soc.***294**, 2 (1986).

[12.44] V. Rom-Kedar, "Transport rates of a class of two-dimensional maps and flows", *Physica D* **43**, 229 (1990);

[12.45] V. Daniels, M. Vallières and J-M. Yuan, "Chaotic scattering on a double well: Periodic orbits, symbolic dynamics, and scaling", *Chaos*, **3**, 475, (1993).

[12.46] P.H. Richter, H.-J. Scholz and A. Wittek, "A Breathing Chaos", *Nonlinearity* **1**, 45 (1990).

[12.47] F. Hofbauer, "Periodic points for piecewise monotone transformations", *Ergod. The. and Dynam Sys.* **5**, 237 (1985).

[12.48] F. Hofbauer, "Piecewise invertible dynamical systems", *Prob. Th. Rel. Fields* **72**, 359 (1986).

[12.49] K.T. Hansen, "Pruning of orbits in 4-disk and hyperbola billiards", *CHAOS* **2**, 71 (1992).

[12.50] G. Troll, "A devil's staircase into chaotic scattering", *Pysica D* **50**, 276 (1991)

[12.51] P. Grassberger, "Toward a quantitative theory of self-generated Complexity", *Int. J. Theor. Phys* **25**, 907 (1986).

[12.52] F. Giovannini and A. Politi, "Generating partitions in Hénon-type maps", *Phys. Lett.* **A 161**, 333 (1992).

[12.53] P. Grassberger, R. Badii and A. Politi, *Scaling laws for invariant measures on hyperbolic and nonhyperbolic attractors*, *J. Stat. Phys.* **51**, 135 (1988).

[12.54] S. Isola and A. Politi, "Universal encoding for unimodal maps", *J. Stat. Phys.* **61**, 259 (1990). Markov diagrams Kai

[12.55] Y. Wang and Huimin Xie, "Grammatical complexity of unimodal maps with eventually periodic kneading sequences", *Nonlinearity* **7**, 1419 (1994).

[12.56] A. Boyarski, M. Skarowsky, *Trans. Am. Math. Soc.* **225**, 243 (1979); A. Boyarski, *J.Stat. Phys.* **50**, 213 (1988).

[12.57] C.S. Hsu, M.C. Kim, *Phys. Rev. A* **31**, 3253 (1985); N. Balmforth, E.A. Spiegel, C. Tresser, *Phys. Rev. Lett.* **72**, 80 (1994).

[12.58] F. Christiansen and A. Politi, "Generating partition for the standard map", *Phys. Rev. E* **51**, R3811 (1995).

[12.59] F. Christiansen and A. Politi, "Symbolic encoding in symplectic maps", *Nonlinearity* **9**, 1623 (1996).

[12.60] F. Christiansen and A. Politi, "Guidelines for the construction of a generating partition in the standard map", *Physica D* **109**, 32 (1997).

[12.61] D.L. Rod, *J. Diff. Equ.* **14**, 129 (1973).

[12.62] R.C. Churchill, G. Pecelli and D.L. Rod, *J. Diff. Equ.* **17**, 329 (1975).

[12.63] R.C. Churchill, G. Pecelli and D.L. Rod, in G. Casati and J. Ford, eds., *Como Conf. Proc. on Stochastic Behavior in Classical and Quantum Hamiltonian Systems* (Springer, Berlin 1976).

[12.64] R. Mainieri, Ph. D. thesis, New York University (Aug 1990); *Phys. Rev.* **A 45**,3580 (1992)

[12.65] M.J. Giannoni and D. Ullmo, "Coding chaotic billiards: I. Non-compact billiards on a negative curvature manifold", *Physica* **D 41**, 371 (1990).

[12.66] D. Ullmo and M.J. Giannoni, "Coding chaotic billiards: II. Compact billiards defined on the psudosphere", *Physica* **D 84**, 329 (1995).

[12.67] H. Solari, M. Natiello and G.B. Mindlin, *"Nonlinear Physics and its Mathematical Tools"*, (IOP Publishing Ltd., Bristol, 1996).

[12.68] R. Gilmore, "Topological analysis of chaotic dynamical systems", submitted to *Rev. Mod. Phys.* (1997).

[12.69] P. Dahlqvist, *On the effect of pruning on the singularity structure of zeta functions*, J. Math. Phys. **38**, 4273 (1997).

⇓PRELIMINARY

[12.70] E. Hille, *Analytic function theory II*, (Ginn and Co., Boston 1962).

[12.71] K.T. Hansen, *Symbolic dynamics of bimodal maps*, in preparation.

[12.72] P. Cvitanović, in *Nonlinear Physical Phenomena, Brasilia 1989 Winter School*, À. Ferraz, F. Oliveira and R. Osorio, eds. (World Scientific, Singapore 1990).

[12.73] P. Cvitanović and K.T. Hansen, "Symbolic dynamics and Markov partitions for stadium billiard", *J. Stat. Phys.* , to appear.

⇑PRELIMINARY